

# LJMU Research Online

Mohanrao, R, Pinto, CS, Suchenko, A, Clarkson, GJ, Wills, M, Roesner, S, Shipman, M and Balasubramanian, MK

Single-Benzene-Based Clickable Fluorophores for In Vitro and In Vivo Bioimaging

https://researchonline.ljmu.ac.uk/id/eprint/27346/

#### Article

**Citation** (please note it is advisable to refer to the publisher's version if you intend to cite from this work)

Mohanrao, R, Pinto, CS, Suchenko, A, Clarkson, GJ, Wills, M, Roesner, S ORCID logoORCID: https://orcid.org/0000-0003-2143-4708, Shipman, M and Balasubramanian, MK (2025) Single-Benzene-Based Clickable Fluorophores for In Vitro and In Vivo Bioimaging. Chemistryselect. 10 (9). e202405738-

LJMU has developed **LJMU Research Online** for users to access the research output of the University more effectively. Copyright © and Moral Rights for the papers on this site are retained by the individual authors and/or other copyright owners. Users may download and/or print one copy of any article(s) in LJMU Research Online to facilitate their private study or for non-commercial research. You may not engage in further distribution of the material or use it for any profit-making activities or any commercial gain.

The version presented here may differ from the published version or from the version of the record. Please see the repository URL above for details on accessing the published version and note that access may require a subscription.

For more information please contact <a href="mailto:researchonline@ljmu.ac.uk">researchonline@ljmu.ac.uk</a>

Check for updates



www.chemistryselect.org

# Single-Benzene-Based Clickable Fluorophores for In Vitro and In Vivo Bioimaging

Raja Mohanrao, [a, b] Clyde S. Pinto, [a] Andrejus Suchenko, [a] Guy J. Clarkson, [b] Martin Wills, [b] Stefan Roesner, \*[b, c] Michael Shipman, \*[b, d] and Mohan K. Balasubramanian \*[a]

A series of miniaturized, clickable single-benzene-based fluorophores derived from tetrafluoroterephthalonitrile is reported. Fluorophores based on a tetrahydroquinoxaline skeleton exhibited improved photophysical properties due to enhanced electron delocalization between donor and acceptor groups com-

pared to those with a dihydro[1,4]thiazine skeleton. These easily synthesized clickable fluorophores were successfully applied in both in vitro and in vivo bioimaging following protein conjuga-

#### 1. Introduction

The ideal properties of fluorophores for bioimaging include compact size, facile synthesis, tunability of absorption and emission wavelengths ranging from UV to far IR, large Stokes shift, high quantum yield, and good solubility in aqueous media.[1] Typically, polyaromatic  $\pi$ -conjugated fluorophores often suffer from poor solubility due to their tendency to aggregate, and they often require complex, multistep synthesis and purification.<sup>[2,3]</sup> Moreover, the presence of a large fluorophore can potentially disrupt the properties and biological function of target molecules.<sup>[4]</sup> Owing to their simple aromatic skeleton, the design and synthesis of single-benzene-based fluorophores (SBBFs) have attracted considerable attention.<sup>[5]</sup> In contrast to large polyaromatic fluorophores, SBBFs contain electron-donor (D)—acceptor (A) functional groups incorporated into a compact benzene ring. [6-13] Because of their facile synthesis, various types of SBBFs have recently been developed and utilized in bioimaging applications.[4,14-17] In addition, their emission can easily be tuned by varying the substituents on the arene ring.[18,19]

Zhang and coworkers reported the simple SBBF precursor tetrafluoroterephthalonitrile (4F-2CN), which was able to efficiently visualize and differentiate the common biological thiols cysteine (Cys), homocysteine (Hcy), and glutathione (GSH) (Figure 1a).[20] The product from the reaction of 4F-2CN with Cys, 2F-2CN-Cys, displayed two-photon fluorescence properties. Subsequently, Huo and coworkers designed the  $\gamma$ -glutamyl transpeptidase (GGT) activated, water-soluble, two-photon fluorescent probe 3F-2CN-GSH. This probe could be cleaved in situ when exposed to GGT-overexpressing cancer cells, forming a fluorophore with a 2F-2CN-Cys skeleton (Figure 1a).[21] Thus, 3F-2CN-GSH has the potential to distinguish cancer cells from normal cells. Taking inspiration from these reports and the work of Banerjee and coworkers, [22,23] we designed a 4F-2CN-based fluorophore, where ring B is made from  $\beta$ -aminoalanine instead of cysteine (Figure 1b).

We hypothesized that nitrogen in the ring would promote greater planarity and conjugation compared to sulfur, leading to increased charge delocalization between the donor and acceptor groups, ultimately enhancing the fluorescence properties.[22-25] Herein, we report the synthesis of four 2F-2CN-Cys and 2F-2CN-(β-NH<sub>2</sub>Ala) analogs appended to maleimide, which are suitable for conjugation to proteins through the thiol-ene click reaction. We assessed their photophysical properties in ethanol and aqueous solution and demonstrated the application of these miniaturized fluorophores in the bioimaging of actin filaments and zebrafish embryos.

- [a] Dr. R. Mohanrao, Dr. C. S. Pinto, Dr. A. Suchenko, Prof. M. K. Balasubramanian Centre for Mechanochemical Cell Biology and Warwick Medical School. Division of Biomedical Science, University of Warwick, CoventryCV4 7AL, UK E-mail: m.k.balasubramanian@warwick.ac.uk
- [b] Dr. R. Mohanrao, Dr. G. J. Clarkson, Prof. M. Wills, Dr. S. Roesner, Prof. M. Shipman Department of Chemistry, University of Warwick, Gibbet Hill Road,

CoventryCV4 7AL, UK

E-mail: s.k.roesner@limu.ac.uk

michael.shipman@durham.ac.uk

School of Pharmacy and Biomolecular Sciences, Liverpool John Moores University, Byrom Street, LiverpoolL3 3AF, UK

[d] Prof. M. Shipman

The Palatine Centre, Durham University, Stockton Road, Durham DH1 3LE,

- Supporting information for this article is available on the WWW under https://doi.org/10.1002/slct.202405738
- © 2025 The Author(s). ChemistrySelect published by Wiley-VCH GmbH. This is an open access article under the terms of the Creative Commons Attribution License, which permits use, distribution and reproduction in any medium, provided the original work is properly cited.

#### 2. Results and Discussion

We first synthesized 2F-2CN-Cys (1)[20] and incorporated a maleimide functional group in three synthetic steps (Scheme 1a). First, carboxylic acid 1 was coupled with Boc-protected amine 2. After further deprotection, the maleimide moiety was incor-

9, Dowlanded from https://chemistry-europe.online/brary.wiley.com/doi/10.1002/sct.202405738 by LIVERPOOL JOHN MOORES UNIV, Wiley Online Library on [15/10/2025]. See the Terms and Conditions (https://online/brary.wiley.com/terms-and-conditions) on Wiley Online Library for rules of use; OA articles are governed by the applicable Creative Commons License

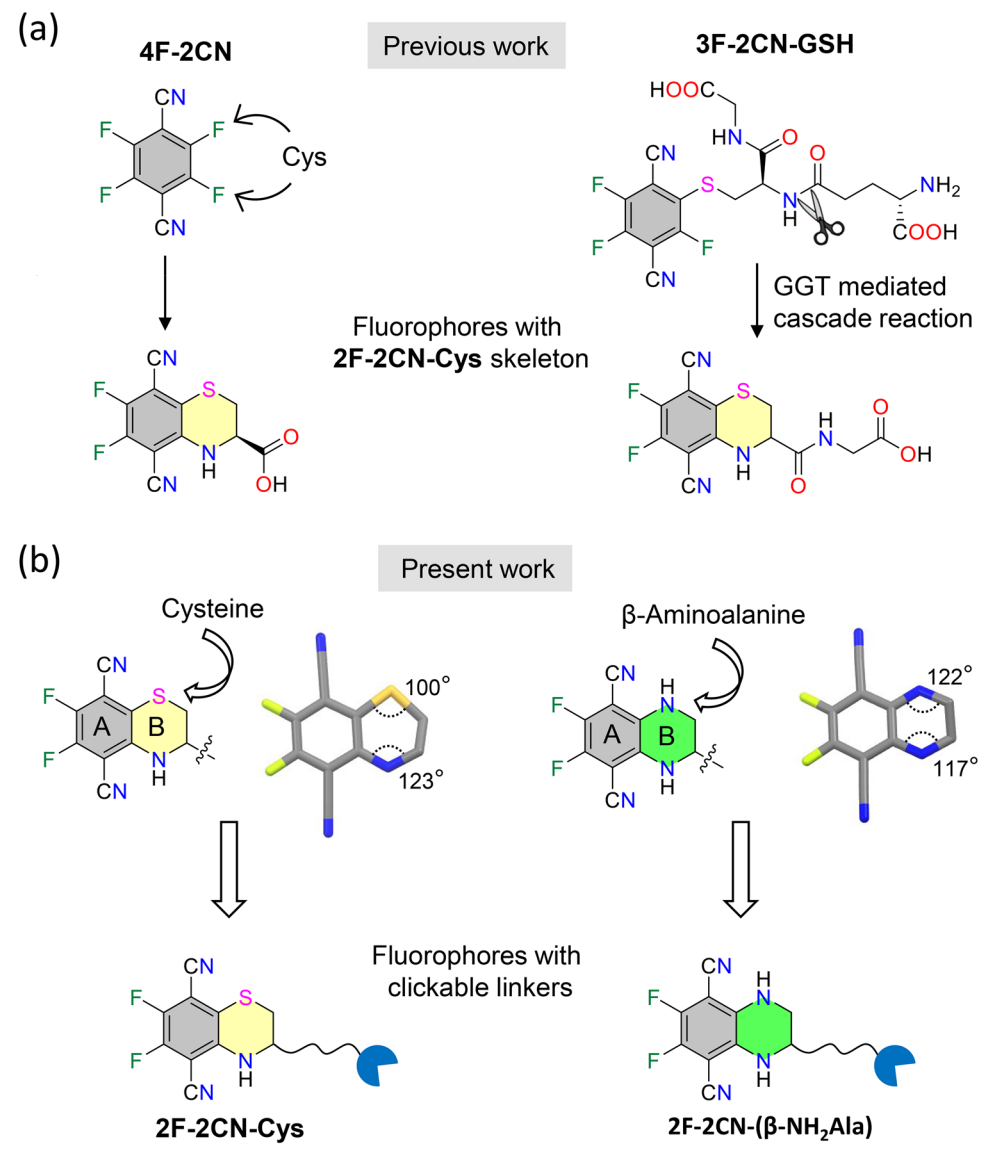


Figure 1. a) Reported fluorophores with 2F-2CN-Cys skeleton. b) This work: Comparison of the 2F-2CN fluorophores based on cysteine and  $\beta$ -aminoalanine and their derivatives with clickable linkers.

porated to obtain fluorophore F1, for which we successfully obtained a crystal structure. [26] The maleimide unit in the SBBF

Scheme 1. Synthesis of fluorophore maleimides F1 and F2.

Scheme 2. Synthesis of fluorophore-triazole-maleimides F3 and F4. (a) Prepared as R-enantiomer.

allows for site-specific thiol-ene click coupling with proteins through thiol-containing amino acids. The  $\beta$ -alanine analog **F2** was synthesized using a similar strategy (Scheme 1b). We prepared the carboxylic acid derivative ( $\pm$ )-5 by treating 4F-2CN

Chemistry Europe

European Chemical Societies Publishing

Figure 2. Crystal structures of a) 1 (reported)<sup>[20]</sup> and b) 9, including bond angles and dihedral angles. Hydrogen atoms are omitted for clarity.

(3) with 1,2-diaminopropionate  $(\pm)$ -4, followed by saponification. Following the same strategy as for F1, the maleimide group was attached to  $(\pm)$ -5 to yield clickable precursor F2. As discussed above, we anticipated that replacing sulfur with nitrogen in F2 would improve planarity and electron delocalization, thereby modifying the photophysical properties of the fluorophore.

In addition, we prepared clickable azide-based fluorophores 6 (crystal structure obtained) and 7 by reacting (R)-1 and ( $\pm$ )-5 with 2-azidoethylamine. These fluorophores were then coupled with maleimide-alkyne 8 using Cu-catalyzed azide-alkyne cycloaddition (CuAAC) chemistry (Scheme 2). The resulting fluorophore maleimides, F3 and F4, containing triazole linkers, were thus also available for further protein conjugation.

We were able to obtain a crystal structure of compound 9,<sup>[26]</sup> the methyl ester of 5, and compared it with the reported solid-

state structure of 1 (Figure 2).<sup>[20]</sup> In compound 1, the bond angles C6-S1-C5 and C7-N3-C4 are 100.1° and 123.0°, respectively, while the dihedral angle of S1-C6-C7-N3 is —2.75°. In comparison, compound 9 exhibits bond angles of 122.1° for C7-N6-C5 and 117.4° for C8-N4-C4, with a dihedral angle of N6-C7-C8-N4 being 1.07°. This indicates that the two nitrogen atoms in 9 adopt a more planar conformation compared to the sulfur–nitrogen combination in fluorophore 1. Recent reports suggest that secondary amines in plane with terephthalonitriles (TN) exhibit enhanced emission properties.<sup>[23]</sup>

Next, we studied the photophysical properties of the fluorophore maleimides F1–F4 in ethanol (Table 1). Absorption spectra showed maxima ( $\lambda_{\text{max,abs}}$ ) between 410 and 415 nm with molar extinction coefficients ( $\varepsilon$ ) ranging from 5300 to 11,305 L mol $^{-1}$  cm $^{-1}$ . The corresponding emission maxima ( $\lambda_{\text{max,em}}$ ) were measured between 480 and 490 nm when excited at  $\lambda_{\text{max,abs}}$ . Quantum yields  $\Phi_{\text{F}}$  ranged from 6.6% for compound F1 up to 18.7% for maleimide F4. For both pairs of compounds, higher quantum yields were measured for the dinitrogen fluorophores F2 and F4 compared to their sulfur-containing counterparts, F1 and F3. [28]

It is well established that a maleimide linker attached to a fluorophore can quench fluorescence through intramolecular charge transfer (ICT) or photoinduced electron transfer (PET) from the fluorophore to the maleimide double bond. [29,30] However, when maleimides react with thiols, the double bond becomes saturated, preventing fluorescence quenching. To examine the impact of protein conjugation via a thiol on fluorophore performance, we coupled maleimide F1 and F2 with cysteine derivative 10 to yield F5 and F6 (Scheme 3). Similar to F1, F5 exhibited nearly identical excitation and emission maxima with a molar extinction coefficient value of 6169 L mol<sup>-1</sup> cm<sup>-1</sup> (Table 1). However, the quantum yield  $(\Phi_F)$  for F5 increased nearly fourfold (23.0%). Similarly, the nitrogen-containing derivative F6 displayed excitation and emission maxima comparable to its precursor **F2**. In this case, the quantum yield  $\Phi_F$  for **F6** was even higher, increasing nearly six-fold to 51.3%.

Next, we measured the photophysical properties of fluorophore derivatives **F1**—**F6** in aqueous solution (Table 2) to assess how these dye molecules would perform in vitro and in vivo imaging. As expected, the absorption maxima ( $\lambda_{\text{max,abs}}$ ) and emission maxima ( $\lambda_{\text{max,em}}$ ) were similar to those in ethanolic solution, ranging from 407 to 413 nm for  $\lambda_{\text{max,abs}}$  and from 488 to 492 nm for  $\lambda_{\text{max,em}}$ . The molar extinction coefficients ( $\varepsilon$ ) in water at

Table 1. Photophysical properties of fluorophore derivatives F1–F6 in EtOH.						
Fluorophore	Abs $\lambda_{max,abs}$ (nm)	Em $\lambda_{\text{max,em}}$ (nm)	Molar Extinction Coefficient $\varepsilon$ (L mol <sup>-1</sup> cm <sup>-1</sup> )	Quantum Yield $\Phi_{\text{F}}^{\text{a}}$		
F1	411	480	11,305	0.066		
F2	415	488	7519	0.086		
F3	410	480	6280	0.079		
F4	415	490	5300	0.187		
F5	411	481	6169	0.230		
F6	414	488	5391	0.513		
$^{\rm a)}$ Calculated with respect to coumarin 6 in ethanol ( $\Phi_{\text{F}}=0.78$ ) as standard. $^{[27]}$						

eithrary.wiley.com/doi/10.1002/slct.202405738 by LIVERPOOL JOHN MOORES UNIV, Wiley Online Library on [15/10/2025]. See the Terms and Conditions (https://onlinelibrary.wiley.com/terms-and-conditions) on Wiley Online Library for rules of use; OA articles are governed by the applicable Creative Common

FOR 
$$H = 10$$
  $H = 10$   $H = 10$ 

Scheme 3. Reaction of fluorophore maleimides F1 and F2 with cysteine derivative 10.

Fluorophore	Abs $\lambda_{max,abs}(nm)$	$Em \ \lambda_{max,em}(nm)$	Molar Extinction Coefficient $\varepsilon$ (L mol $^{-1}$ cm $^{-1}$ )	Quantum Yield $\Phi_{\text{F}}^{\text{a)}}$
F1	410	488	5568	0.060
F2	410	492	2494	0.076
F3	410	490	2731	0.109
F4	412	491	3110	0.150
F5	413	490	5112	0.166
F6	407	490	1956	0.169

Calculated with respect to coumarin 6 in ethanol ( $\Phi_F = 0.78$ ) as standard applying the refraction indexes of water and EtOH.

 $\lambda_{max,abs}$ , however, were significantly lower than those measured in ethanol. For example, while  $\varepsilon$  in ethanol ( $\varepsilon_{\text{EtOH}}$ ) for fluorophore **F1** was measured at 11,305 L mol<sup>-1</sup> cm<sup>-1</sup>, the value in water ( $\varepsilon_{\text{water}}$ ) for the same compound was approximately halved to 5568 L mol<sup>-1</sup> cm<sup>-1</sup>. This trend was consistent across all fluorophores. Finally, we determined the quantum yields  $(\Phi_F)$  for compounds F1-F6 in aqueous solution. For F1-F4, the quantum yield values were similar to those in ethanol. However, while thiol coupling for F5 and F6 resulted in a notable increase in quantum efficiency in ethanol (see Table 1), this increase in water was only moderate, with  $\Phi_F$  values of 16.6% for **F5** (compared to 23.0% in ethanol) and 16.9% for F6 (compared to 51.6% in ethanol). Overall, while the fluorophores displayed reasonable photophysical properties in aqueous solution, their properties as fluorescent dyes were enhanced in ethanol.

To assess the potential of these fluorescent small molecules for in vitro and in vivo protein bioimaging, we developed two assays. In the first assay, we labelled the cytoskeletal protein human  $\beta$ -actin, which assembles into filamentous polymers. [31,32] Filaments composed of monomeric actins can be readily visualized using conventional epifluorescence and/or total internal reflection microscopy. Purified  $\beta$ -actin was polymerized and subsequently labelled with compounds F1-F4 through specific reaction of the native Cys 374 residue in actin with the maleimide moiety of F1-F4.[33] Actin bound to F1, F2, F3, and F4 was polymerized in vitro and imaged by spinning disk confocal microscopy. The fluorophores were excited with a 405 nm laser, and emissions were recorded using an EMCCD camera through a GFP emission filter, allowing detection wavelengths of 505 nm and above.<sup>[34]</sup> Under these imaging conditions, polymers labelled with compounds F2 and F4 were readily detectable (Figure 3). In contrast, those labelled with compound F1 showed weaker fluorescence, and the signal from filaments labelled with compound F3 was below detectable levels. The fluorescence intensities of filaments labelled with compounds F1, F2, and F4 were 1024, 2112, and 1286 RFU, respectively.[28]

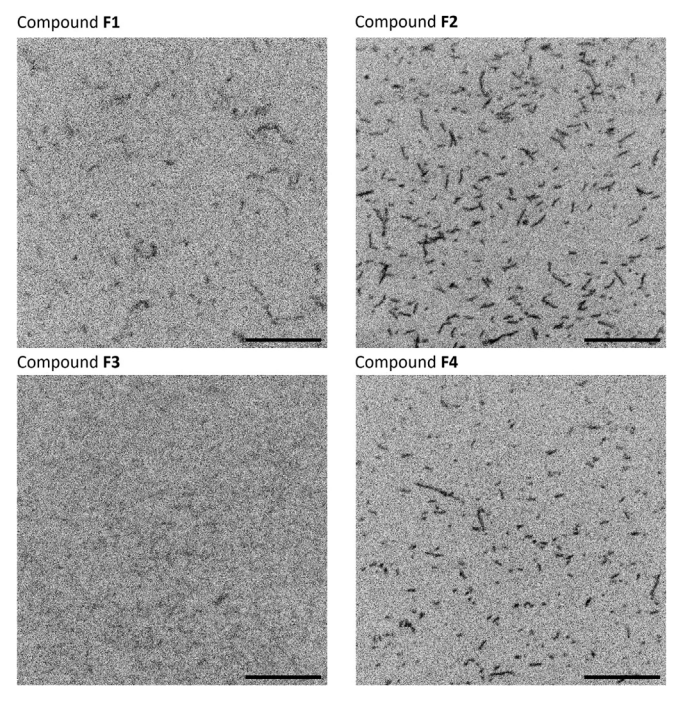


Figure 3. In vitro imaging of actin filaments excited at 405 nm and labelled with compounds F1, F2, F3, and F4. Purified  $\beta$ -actin proteins labelled with fluorescent compounds were polymerized. The filaments were imaged with a spinning disk confocal fluorescence microscope. Scale bars are 10 µm. [28]

As our in vitro experiments with labelled actin showed that compound F2 was the best suited for imaging proteins and protein assemblies, we selected it for further in vivo testing. Zebrafish embryos were chosen for these experiments due to their optical transparency and ease of injection, which allowed for protein introduction and live visualization (Figure 4a).[34] First, we injected embryos with actin protein labelled with F2 (see Figure S3 in the Supporting Information) and observed fluorescence at cellular margins, likely corresponding to cell

from https://chemistry-europe.onlinelibrary.wiley.com/doi/10.1002/slct.202405738 by LIVERPOOL JOHN MOORES UNIV, Wiley Online Library on [15/10/2025]. See the Terms and Conditions (https://onlinelibrary.wiley.com/nerms-

and-conditions) on Wiley Online Library for rules of use; OA articles are governed by the applicable Creative Commons

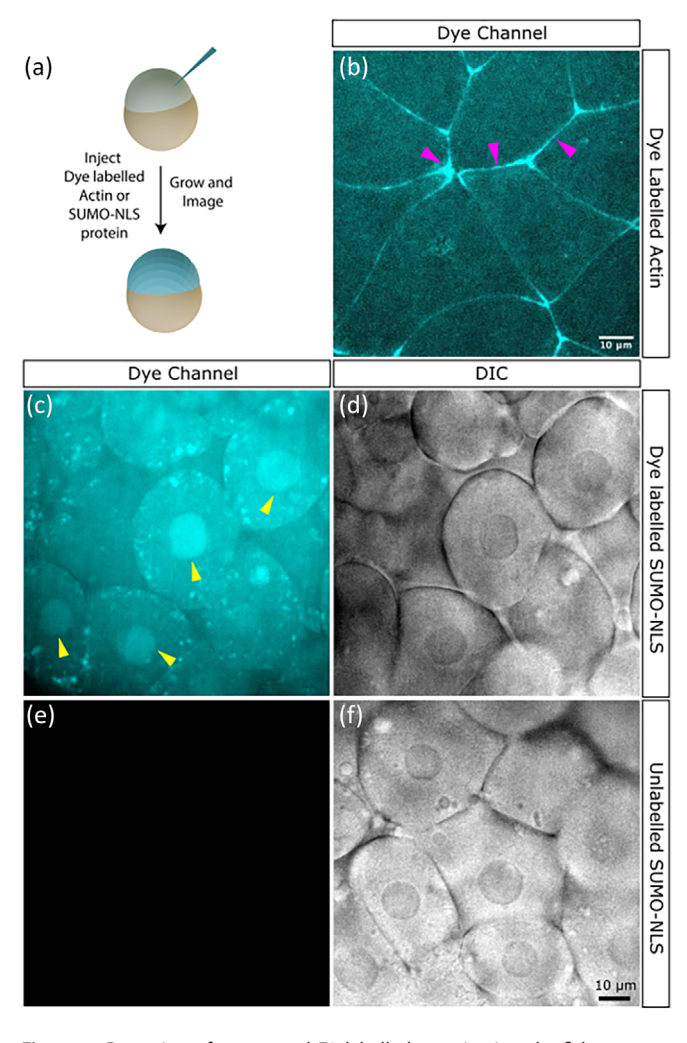


Figure 4. Detection of compound F2 labelled proteins in zebrafish embryos. a) Schematic of the experimental paradigm used to test the detectability of compound F2 labelled proteins in vivo. b) Zebrafish embryos were injected with compound F2 dye labelled actin and imaged using an excitation wavelength of 405 nm and emission wavelength of 505 nm and above. Magenta arrowheads indicate staining observed at cellular junctions. c-f) Zebrafish embryos were injected with compound F2 dye labelled (c and d) or unlabelled (e and f) SUMO-NLS protein. The dye channel (c and e) at the same settings for labelled and unlabelled protein and corresponding DIC channel (d and f) are shown. The yellow arrowheads in c show the location of nuclear structures as seen in the DIC channel d. The scale bars in b and f are 10 um.

junctions (Figure 4b). To confirm that the observed protein localization was not an artefact of labelling, we tested a protein target to a different cellular location, namely the nucleus. We designed a construct containing a small ubiquitin-like modifier (SUMO) tag for purification, fused to two SV40 nuclear localization signals (NLS), with three cysteines engineered into this cysteine-light NLS sequence for maleimide coupling. After purifying and labelling this protein with F2 (see Figure S3), we injected it into embryos. The dye-labelled SUMO-NLS protein displayed clear nuclear staining observed via differential interference contrast (DIC) imaging (Figure 4c,d). By contrast, embryos injected with unlabeled SUMO-NLS protein displayed minimal autofluorescence, undetectable at the imaging settings used for dye-labelled samples (Figure 4e,f). Taken together, these pre-

liminary studies demonstrate that proteins can be effectively labelled with fluorophore **F2**, retaining both function and in vivo detectability.

#### 3. Conclusion

In conclusion, we have designed and synthesized clickable single-benzene-based fluorophores, 2F-2CN-Cys and 2F-2CN- $(\beta-NH_2Ala)$ . By substituting the ring heteroatom from sulfur (dihydro[1,4]thiazine skeleton) to nitrogen (tetrahydroquinoxaline skeleton), we were able to improve the photophysical properties of the resulting SBBF dyes. The maleimide group enabled conjugation of the fluorophores to actin filaments via thiol-ene click reaction. Using these compounds, we successfully labelled and visualized actin both in vitro and in vivo assays. Actin and SUMO-NLS proteins labelled with the 2F-2CN-(β-NH<sub>2</sub>Ala)-based fluorophore F2 localized to their expected positions in zebrafish embryos in vivo. To the best of our knowledge, this is the first example of single benzene-based fluorophores coupled to a protein for bioimaging. Studies on the incorporation of the parent fluorophore amino acids 2F-2CN-Cys and 2F-2CN-(β-NH<sub>2</sub>Ala) into proteins through genetic code expansion are ongoing in our laboratory.[36]

# **Supporting Information**

The authors have cited additional references within the Supporting Information.<sup>[37–41]</sup>

## Acknowledgements

Mohan K. Balasubramanian was funded by Wellcome Trust (101885/C/13/Z), ERC-Actomyosin Ring (GA 671083), and Wellcome Trust (203276/B/16/Z). We thank the University of Warwick for financial support and all members of the Shipman, Wills, and Balasubramanian laboratories for discussion and critical feedback.

### **Conflict of Interests**

The authors declare no conflict of interest.

#### **Data Availability Statement**

The data that support the findings of this study are available in the supplementary material of this article.

**Keywords:** Bioconjugates • Bioimaging • Chromophores • Fluorescent probes • Single-benzene fluorophores

[1] a) Z. Li, P.-Z. Liang, T.-B. Ren, L. Yuan, X.-B. Zhang, Angew. Chem., Int. Ed. 2023, 62, e202305742; b) Angew. Chem. 2023, 135, e202305742.



- [2] K. Li, T.-B. Ren, S. Huan, L. Yuan, X.-B. Zhang, J. Am. Chem. Soc. 2021, 143, 21143
- [3] a) T. Beppu, K. Tomiguchi, A. Masuhara, Y.-J. Pu, H. Katagiri, *Angew. Chem., Int. Ed.* **2015**, *54*, 7332-7335; b) *Angew. Chem.* **2015**, *127*, 7443.
- [4] a) S. Benson, F. de Moliner, W. Tipping, M. Vendrell, Angew. Chem., Int. Ed. 2022, 61, e202204788; b) Angew. Chem. 2022, 134, e202204788.
- [5] F. de Moliner, F. Nadal-Bufi, M. Vendrell, Curr. Opin. Chem. Biol. 2024, 80, 102458.
- [6] S. Sarkar, A. Shil, Y. W. Jun, Y. J. Yang, W. Choi, S. Singha, K. H. Ahn, Adv. Funct. Mater. 2023, 33, 2304507.
- [7] H. Kim, Y. Kim, D. Lee, Acc. Chem. Res. 2024, 57, 140.
- [8] a) M. Shimizu, Y. Takeda, M. Higashi, T. Hiyama, Angew. Chem., Int. Ed. 2009, 48, 3653–3656. b) Angew. Chem. 2009, 121, 3707.
- [9] Y. Okada, M. Sugai, K. Chiba, J. Org. Chem. 2016, 81, 10922.
- [10] R. Huang, B. Liu, C. Wang, Y. Wang, H. Zhang, J. Phys. Chem. C 2018, 122, 10510
- [11] J. Christoffers, Eur. J. Org. Chem. 2018, 2018, 2366-2377.
- [12] B. Liu, Q. Di, W. Liu, C. Wang, Y. Wang, H. Zhng, J. Phys. Chem. Lett. 2019, 10, 1437.
- [13] a) B. Tang, C. Wang, Y. Wang, H. Zhang, Angew. Chem., Int. Ed. 2017, 56, 12543; b) Angew. Chem. 2017, 129, 12717.
- [14] H. M. Kim, B. R. Cho, Chem. Rev. 2015, 115, 5014.
- [15] Y. Jung, J. H. Jin, Y. Kim, J. H. Oh, H. Moon, H. Jeong, J. Kim, Y. K. Park, Y. Oh, S. Park, D. Kim, Org. Bimol. Chem. 2022, 20, 5423.
- [16] X. Liu, R. Huang, Q. Qiao, D. Seah, T. Shen, X. Wu, F. de Moliner, C. Wang, N. Ding, W. Chi, H. Sun, M. Vendrell, Z. Xu, Y. Fang, Precision Molecular Engineering of Miniaturized Near-Infrared Fluorophores for Bioimaging, 13 October 2024, PREPRINT (Version 1) available at Research Square, https://doi.org/10.21203/rs.3.rs-5098198/v1.
- [17] Y. Jin, Z. Wang, M. Dong, P. Sun, W. Chi, Spectrochim. Acta A 2025, 326, 125213.
- [18] J. Kim, J. H. Oh, D. Kim, Org. Biomol. Chem. 2021, 19, 933.
- [19] Z. Xiang, Z.-Y. Wang, T.-B. Ren, W. Xu, Y.-P. Liu, X.-X. Zhang, P. Wu, L. Yuan, X.-B. Zhang, Chem. Commun. 2019, 55, 11462.
- [20] H. Zhang, R. Liu, J. Liu, L. Li, P. Wang, S. Q. Yao, Z. Xu, H. Sun, Chem. Sci. 2016, 7, 256.
- [21] R. Huo, X. Zheng, W. Liu, L. Zhang, J. Wu, F. Li, W. Zhang, C.-S. Lee, P. Wang, Chem. Commun. 2020, 56, 10902.
- [22] A. A. Phadte, A. Chattopadhyay, S. Banerjee, D. S. Sisodiya, T. Raghava, ChemistrySelect 2020, 5, 10177.

- [23] T. Raghava, S. Banerjee, A. Chattopadhyay, J. Org. Chem. 2023, 88, 15708.
- [24] J.-S. Yang, S.-Y. Chiou, K.-L. Liau, J. Am. Chem. Soc. 2002, 124, 2518.
- [25] S. V. K. Isukapalli, P. Pushparajan, S. R. Vennapusa, J. Phys. Chem. A 2022, 126, 1114
- [26] Deposition number 2295310 (for 6), 2295311 (for 9), 2295312 (for 12), and 2295313 (for F1) contain the supplementary crystallographic data for this paper. These data are provided free of charge by the joint Cambridge Crystallographic Data Centre and Fachinformationszentrum Karlsruhe Access Structures service.
- [27] G. A. Reynolds, K. H. Drexhage, Opt. Commun. 1975, 13, 222.
- [28] See the Supporting Information for a detailed description.
- [29] H. Peng, W. Chen, Y. Cheng, L. Hanuka, R. Strongin, B. Wang, Sensors 2012, 12, 15907.
- [30] J. Qian, G. Zhang, J. Cui, L. Zhou, Z. Chen, Z. Zhang, W. Zhang, Sens. Acutators B Chem. 2020, 311, 127923.
- [31] T. D. Pollard, Cold Spring Harb. Perspect. Biol. 2016, 8, a018226.
- [32] T. Hatano, L. Sivashanmugam, A. Suchenko, H. Hussain, M. K. Balasubramanian, J. Cell Sci. 2020, 133, jcs241406.
- [33] a) D. S. Kudryashov, M. Phillips, E. Reisler, Biophys. J. 2004, 87, 1136; b) C. K. Chen, S. A. Benchaar, M. Phan, E. E. Grintsevich, R. R. O. Loo, J. A. Loo, E. Reisler, Biochemistry 2013, 52, 5503.
- [34] C. S. Pinto, M. Mishima, K. Sampath, Histochem. Cell Biol. 2020, 154, 481.
- [35] J. Lu, T. Wu, B. Zhang, S. Liu, W. Song, J. Qiao, H. Ruan, Cell Commun. Signal. 2021, 19, 60.
- [36] R. Mohanrao, C. S. Pinto, A. Suchenko, G. J. Clarkson, M. Wills, S. Roesner, M. Shipman, M. K. Balasubramanian, ChemRxiv preprint 2024, https://doi.org/10.26434/chemrxiv-2024-s1fzw.
- [37] J. Wang, M. Uttamchandani, J. Li, M. Huand, S. Q. Yao, Chem. Commun. 2006, 3783–3785.
- [38] R. Sanichar, J. C. Vederas, Org. Lett. 2017, 19, 1950.
- [39] A. Zaucker, C. A. Mitchell, H. L. E. Coker, K. Sampath, Front. Cell Dev. Biol. 2021, 9, 712503.
- [40] O. V. Dolomanov, L. J. Bourhis, R. L. Gildea, J. A. K. Howard, H. Puschmann, J. Appl. Cryst. 2009, 42, 339.
- [41] G. M. Sheldrick, Acta Cryst. 2015, A71, 3.

Manuscript received: December 6, 2024